nature water

Article

https://doi.org/10.1038/s44221-024-00291-w

# Upwind moisture supply increases risk to water security

Received: 24 October 2023

Accepted: 15 July 2024

Published online: 02 September 2024

Check for updates

José Posada-Marín [1,2,3] ✉, Juan Salazar [1], Maria Cristina Rulli [4], Lan Wang-Erlandsson [5,6,7] & Fernando Jaramillo [2]

Transboundary assessments of water security typically adopt an 'upstream' perspective, focusing on hazards and vulnerabilities occurring within a given hydrological basin. However, as the moisture that provides precipitation in the hydrological basin probably originates 'upwind', hazards and vulnerabilities potentially altering the moisture supply can be overlooked. Here we perform a global assessment of risk to water security in 379 hydrological basins accounting for upwind vulnerabilities and hazards from limited governance and environmental performance. We compare this upwind assessment with the more conventional approach focusing upstream. We find that accounting for upwind moisture supply increases the assessed risk to water security. The upwind perspective results in 32,900 $km^3\ yr^{-1}$ of water requirements (that is, the specific water needs of vegetation for their development) under very high risk, compared with 20,500 $km^3\ yr^{-1}$ under the upstream perspective. This study pinpoints the need to account for upwind moisture dependencies in global water-related risk assessments.

Globally, around 40% of continental precipitation originates in evaporation from land[1]. This amount increases to 80–90% in some regions in Eurasia, South America and Africa[2]. Hence, precipitation over large parts of the Earth's land surface can be vulnerable to upwind changes in the amount and timing of evaporation entering the atmosphere[3–5]. Land and water use related to human activities for food and energy production are known to alter such evaporation[6–10]. For instance, irrigation has been found to increase precipitation downwind, while deforestation decreases it[11–18]. Upwind loss in evaporation can result in loss in downwind precipitation with impacts on agricultural[12,19–22] and hydropower[23], water availability in surface and groundwater resources[19], aquatic and terrestrial ecosystems[24–26] and the livelihoods of many urban and rural communities[27].

These implications have led to calls to include atmospheric water flows in transboundary water management and decision-making[28,29]. Other calls insist on their inclusion in international law[30] and broader water governance frameworks[28,31–33]. For instance, political instability can weaken the control of illegal practices fuelling environmental degradation, such as illicit agricultural expansion and mining[34]. The lack of land and water governance and a weak environmental performance can lead to deforestation[35] and the disappearance of ecosystems that are key for atmospheric moisture supply. As another example, a lack of voice and accountability implies a disregard for citizens in the control or curve of environmental degradation that may lead to modifications of vapour flows[36].

Risk to water security—that is, the human capacity to ensure reliable access to safe and sufficient water resources—is typically calculated as the product of the hazard (natural or human-induced events causing harm), vulnerability (physical susceptibility to adverse effects) and exposure (elements at risk of being affected)[37]. Risk estimates usually account for upstream hazards in the hydrological basin[38–40]. The risks relate to downstream implications of decreasing water supply

[1]GIGA, Escuela Ambiental, Facultad de Ingeniería, Universidad de Antioquia, Medellín, Colombia. [2]Department of Physical Geography/Bolin Centre for Climate Research, Stockholm University, Stockholm, Sweden. [3]Grupo de Investigación en Innovación Digital y Desarrollo Social, IU Digital de Antioquia, Medellín, Colombia. [4]Department of Civil and Environmental Engineering, Politecnico di Milano, Milan, Italy. [5]Stockholm Resilience Centre, Stockholm University, Stockholm, Sweden. [6]Anthropocene Laboratory, the Royal Swedish Academy of Sciences, Stockholm, Sweden. [7]Potsdam Institute for Climate Impact Research, Member of the Leibnitz Association, Potsdam, Germany. ✉e-mail: jose.posada@iudigital.edu.co

https://doi.org/10.1038/s44221-024-00291-w

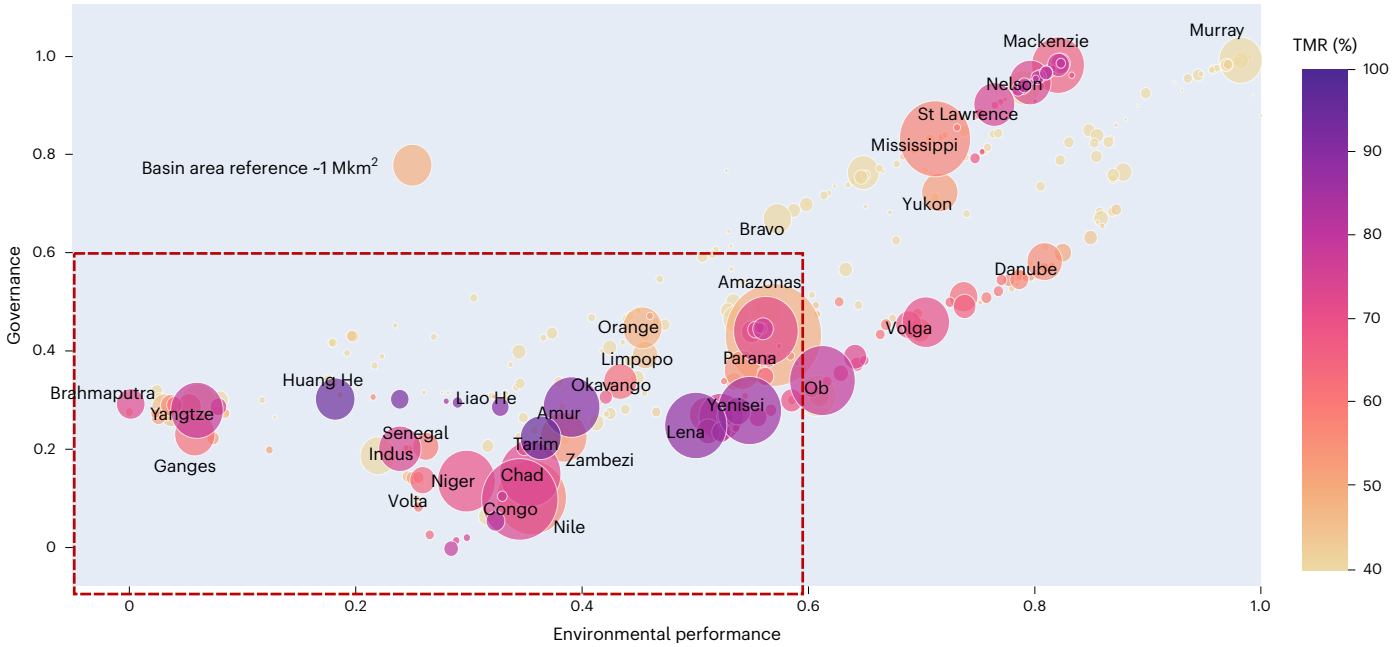


**Fig. 1 | Relationship between the main variables analysed in this study.** The relationship between governance (*y* axis), environmental performance (*x* axis), TMR ratios (colour gradient) and the area of the basin (size of the circle). Governance is calculated as the mean of the five governance indicators (voice accountability, political stability, government effectiveness, regulatory quality and the rule of law; Supplementary Fig. 2a) reported by the World Bank[87] and area-weighted on the basis of the countries lying within the precipitationshed of each hydrological basin. Similarly, environmental performance is given by the 40 indicators of the Environmental Performance Index (Supplementary Fig. 2b) from the Yale Center for Environmental Law and Policy[88]. The dashed red polygon highlights basins with low levels of upwind governance and environmental performance.

in rivers[41], mountain glaciers[42], lakes[43], wetlands[44], aquifers[45,46] and even soil moisture[40]. Yet, recent studies have also included the vulnerabilities and exposures arising from upwind dependencies for water security[27,32]. For instance, Keys et al.[27] merged upstream and upwind dependencies to estimate the integrated water supply vulnerability for 29 megacities. The growing interest in accounting for upwind dependencies for risk assessment matters as precipitation over a hydrologic basin depends on terrestrial moisture recycling (TMR), the mechanism by which upwind evaporation feeds downwind precipitation either within a hydrological basin (local moisture recycling) or across different basins. The dependency can increase or decrease the risk of natural vegetation and crops not receiving the required supply of freshwater[47–50].

Here we build on previous studies that consider the upwind vulnerability of freshwater supply[27,32,33] to analyse global risks to water security. Our main aim is to quantify how accounting for upwind dependencies arising from governance and environmental performance affects the risk in 379 worldwide basins. We estimate risk from two perspectives; the first, 'upstream', is based on political, geographical, ecosystemic and hydroclimatic conditions in the countries sharing the hydrological basin. The second perspective, named 'upwind', relates to the countries sharing the hydrological basin's precipitationshed[20], the upwind continental regions contributing moisture. We consider the freshwater requirements of vegetation and crops within the basin as the most representative exposed asset for basin-scale water security.

We identified 379 large hydrological basins (greater than 3,400 km$^2$) covering 85 Mkm$^2$ whose precipitationsheds extend across more than one country. We refer to these basins as upwind transboundary basins in contrast to the typical definition of upstream transboundary (that is, the hydrological basin is shared by several countries). Around one-third of these upwind transboundary basins (153) are also upstream transboundary. From these upwind transboundary basins, the ones with the highest TMR and, thus, high upwind continental moisture dependency include the Tarim, Huang He, Amur, Yenisei and Lena River basins (Fig. 1). The TMR ratio can indicate how susceptible the water availability of a given hydrological basin is to changes in upwind moisture supply. For instance, a basin depending solely on moisture transport from the ocean would not be affected by any change in land use as long as atmospheric moisture convergence is not affected. Conversely, a basin depending only on continental moisture is subject to any potential change in moisture supply resulting from land use changes.

Most large basins typically have high TMR and low governance values (that is, less than 0.6). Interestingly, the hydrological basins with the highest TMR range between 0 and 0.6 of the maximum governance that can be obtained, pointing to low governability. The Congo River Basin is an example of a large basin with low governance and environmental performance. The water requirements of the Congo River Basin (Supplementary Fig. 1) have a high dependency on land cover changes occurring upwind; its TMR ratio reaches ~73%, and most of the moisture precipitating in the basin has a terrestrial origin, covering countries such as South Sudan, Central African Republic, Congo, Angola and the Democratic Republic of the Congo. Concern about the moisture dependency of the Congo River Basin arises as the low governance and environmental performance of the countries in its precipitationshed (Supplementary Fig. 2) may imply potential hazards to water security. Risks may arise from, for instance, threats of deforestation within the precipitationshed, which can potentially reduce upwind moisture flows, or uncontrolled irrigation, which may increase them[4].

The first component of risk is the hazard. The potential hazard resulting after combining aspects of governance and environmental performance (Methods and Supplementary Fig. 2) depends on whether these aspects are analysed for the upwind (within the precipitationshed) or upstream (within the hydrological basin) countries (Fig. 2a,b). We can identify from both perspectives the highest hazard values in Africa, the Middle East and Asia from the combination of very low to

https://doi.org/10.1038/s44221-024-00291-w

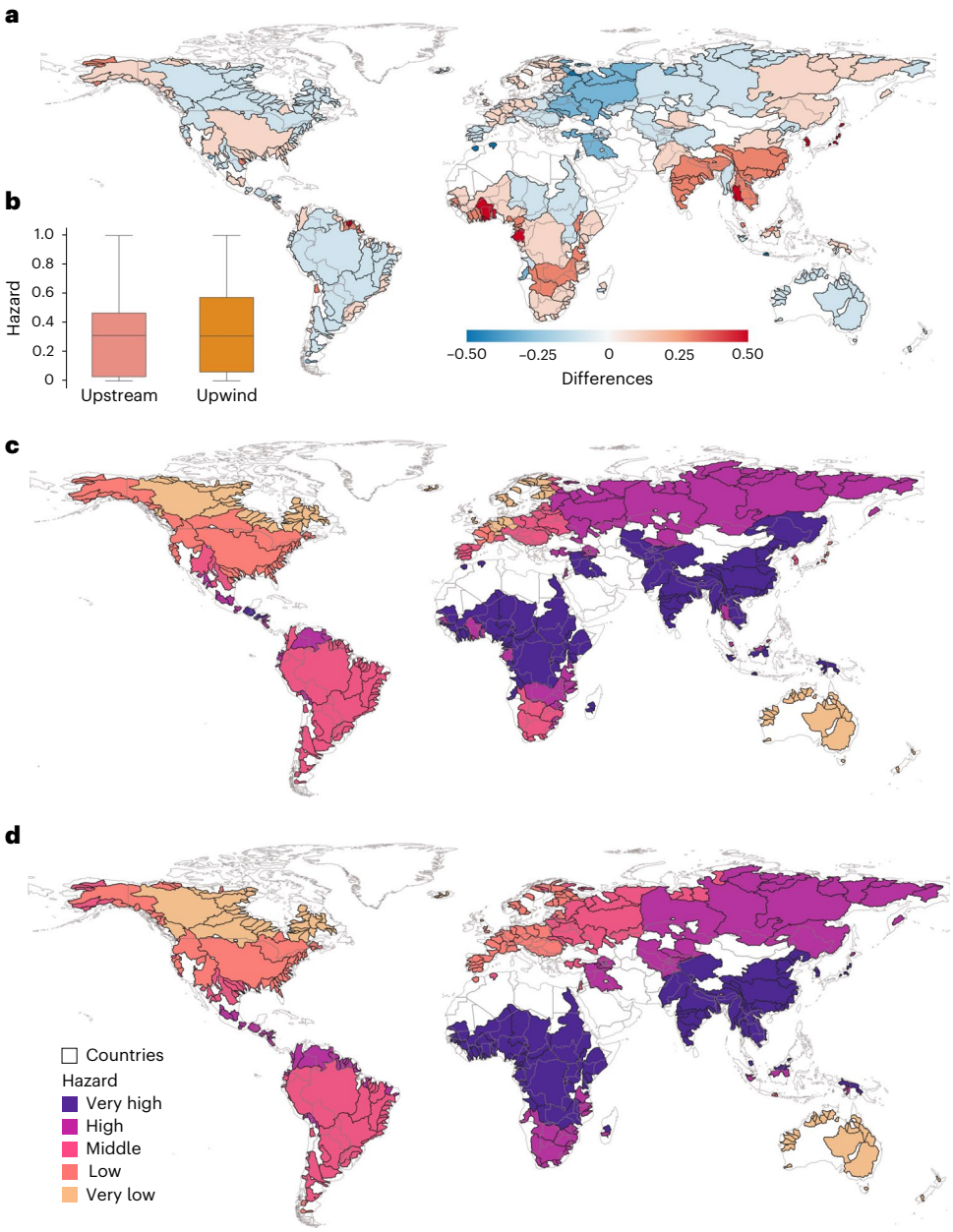


**Fig. 2 | Hazard estimations from risk perspectives. a**, The difference between the hazard estimates of the upwind and upstream perspectives (upwind minus upstream). **b**, A comparison of the distribution of hazards (box plots) of the 379 upwind transboundary basins when including countries in their hydrological basins (upstream) and their precipitationsheds (upwind). In the upstream (upwind) perspective, the minimum value recorded is 0.0 (0.0) and the maximum value is 1.0 (1.0). The centre of the box plot, representing the median of the data, is 0.31 (0.31). The bounds of the box are defined by the first quartile (Q1) and the third quartile (Q3), which are 0.03 (0.06) and 0.47 (0.58), respectively. The whiskers extend to the minimum and maximum values of the distributions. The samples were compared with a one-sided unpaired Wilcoxon rank-sum test to determine the statistical significance of the difference between both perspectives (*P* value 0.25; Wilcoxon rank-sum test). **c**,**d**, The five categories (very high, high, middle, low and very low) are based on min–max normalized values of the hazard after separation in quantiles for the upstream (**c**) and upwind (**d**) perspectives.

middle values of governance and environmental performance (Fig. 2c,d and Supplementary Fig. 2). In African and Middle Eastern countries, the hazard is mainly related to low governance values (Supplementary Fig. 2a), while in Asian countries, it is due to low environmental performance (Supplementary Fig. 2b). We find that the mean global difference between assessing hazard from an upwind and upstream perspective is not statistically significant at the global scale ($P > 0.05$, Wilcoxon rank-sum test; Fig. 2b); a similar number of basins increase or decrease their hazard. Several hydrological basins in Asia (for example, the Yangtze, Ganges and Krishna River basins) and Africa (for example, the Volta, Ogooue and Zambezi River basins) tend to increase their hazards the most when applying an upwind perspective (Fig. 2a). In contrast, some eastern Europe basins experience the most decrease (for example, the Volga, Dniepr and Neva River basins).

The second risk component is the exposure of the asset at risk, that is, the total water requirements for vegetation and crops within the hydrological basin. The Amazon and Congo basins also have some of the largest total water exposure to hazards due to the large freshwater requirements of vegetation within them (Supplementary Fig. 1a). Hence, a higher water requirements implies a larger exposure to upwind/upstream moisture supply changes. These requirements comprise both green water (GW)—the precipitation on land temporarily

https://doi.org/10.1038/s44221-024-00291-w

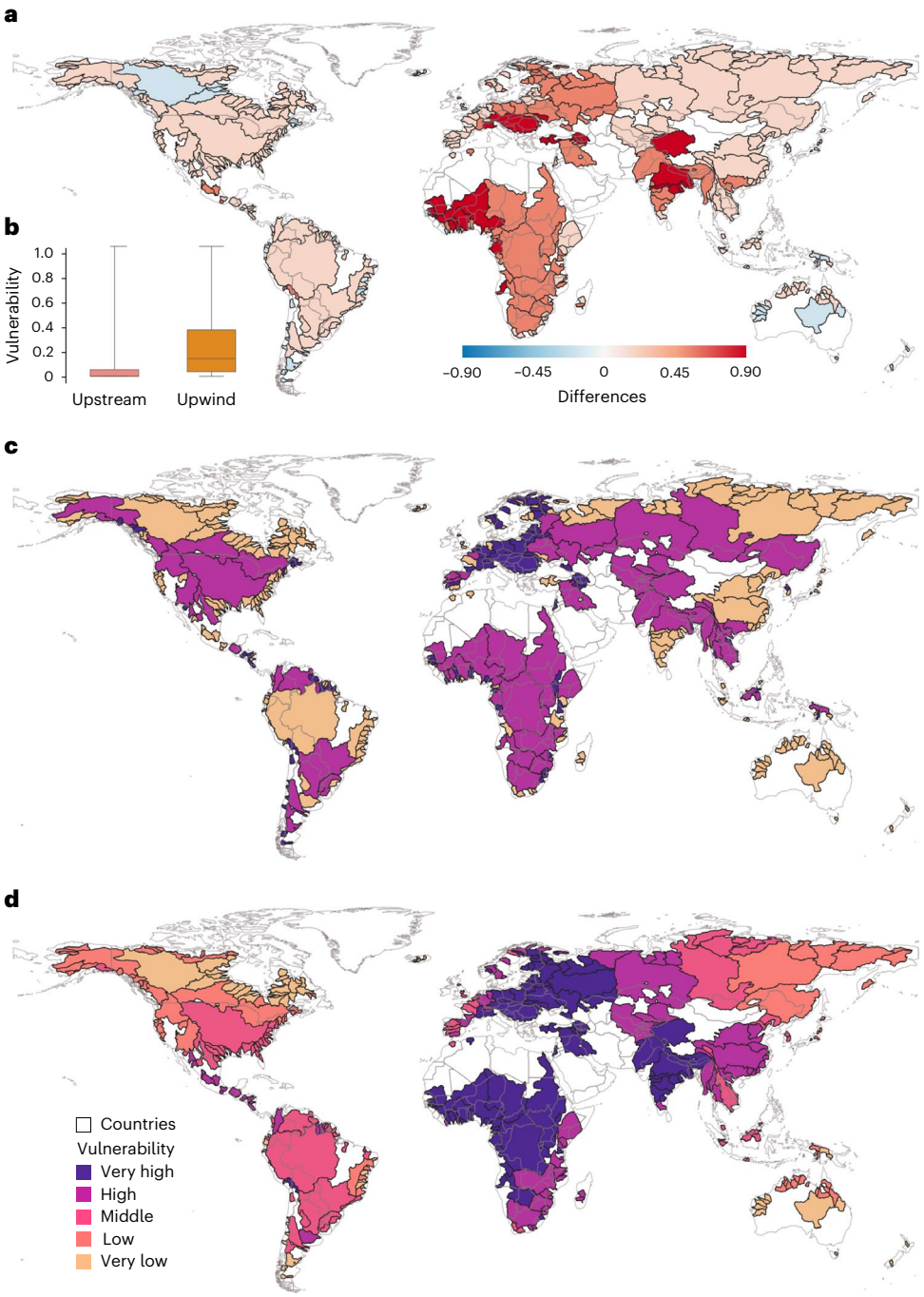


**Fig. 3 | Geophysical vulnerability estimations from risk perspectives.** **a**, Geophysical vulnerability differences between perspectives (upwind minus upstream). **b**, The vulnerability distribution (box plots) for the 379 hydrological basins with transboundary precipitationsheds by perspective. In the upstream (upwind) perspective, the minimum value recorded is 0.0 (0.0) and the maximum value is 1.0 (1.0). The centre of the box plot, representing the median of the data, is 0.00 (0.14). The bounds of the box are defined by the first quartile (Q1) and the third quartile (Q3), which are 0.00 (0.04) and 0.05 (0.36), respectively. The whiskers extend to the minimum and maximum values of the distributions. The samples were compared with a one-sided unpaired Wilcoxon rank-sum test to determine statistical significance in differences ($P$ value $3.88 \times 10^{-55}$). **c**,**d**, Once normalized using a min–max normalization, these values are divided into five categories: very high, high, middle, low and very low, using the quantiles of their distribution for both upstream (**c**) and upwind (**d**) perspectives.

stored in soil and consumed by vegetation (Supplementary Fig. 1b)—and blue water (BW)—freshwater in lakes, rivers and aquifers, mainly consumed in irrigated agriculture (Supplementary Fig. 1c). The total GW and BW requirements in the upwind transboundary basins reaches 40,600 $km^3\ yr^{-1}$ globally.

The third risk component, vulnerability (Fig. 3 and Supplementary Figs. 3 and 4), is the natural susceptibility to adverse effects. Vulnerability results are higher when considering the areas and countries within the precipitationshed than those within the hydrological basin. Contrary to the hazard, the vulnerability shows statistically significant differences between the upwind and upstream perspectives at the global scale (Wilcoxon rank-sum test, $P < 0.05$; Fig. 3a,b). Around 88% of the upwind transboundary basins increase their vulnerability when shifting from an upstream to an upwind perspective of risk (Fig. 3a). The most marked differences occur in Europe (for example, the Danube, Volga, Dniepr and Po River basins), Asia

https://doi.org/10.1038/s44221-024-00291-w

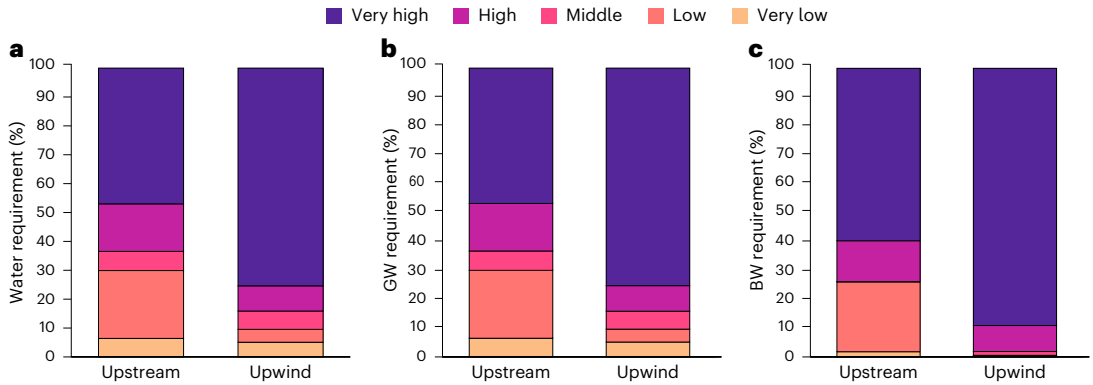


**Fig. 4 | Differences in risk in terms of water requirements between perspectives. a**–**c**, The relative amount of total water (**a**), GW (**b**) and BW (**c**) requirements for each perspective and in each of the five risk categories in all hydrological basins. For example, 89% of BW requirements are at a very high risk when upwind conditions are considered.

(for example, the Tarim, Ganges, Indus and Narmada River basins) and Africa (for example, the Niger, Senegal, Ogooue and Volta River basins).

The mean global increase in vulnerability results from a mean global increase in interdependency ($P < 0.05$, Wilcox rank-sum test; Supplementary Fig. 5d) that is more influential to the score of vulnerability than the global mean decrease in fragility ($P < 0.05$, Wilcox rank-sum test; Supplementary Fig. 5b). Interdependency refers to the number of countries within the basin or precipitationshed, depending on the perspective, assuming that it will be easier to establish management measures and cooperation in water policy if the number of countries is low. Likewise, fragility relates to the area of the hydrological basin or precipitationshed, assuming that the capacity to meet the freshwater requirements at the scale of the hydrological basin is more fragile in smaller surface areas. Furthermore, it is worth noting that most of the basins experiencing higher vulnerabilities from an upwind perspective have relatively large TMR ratios, highlighting their dependency on continental moisture flows originating upwind. Changes in the magnitude of vulnerability between perspectives lead to a reassessment of the vulnerability categories (Fig. 3c,d). For instance, the Amazon, Danube, Congo, Nile, Ganges and Yangtze increase their vulnerability from lower to higher levels when the upwind dependency is accounted for. Overall, the hydrological basins in Africa, the Middle East, Eastern Europe and the Indian Peninsula increase their vulnerability to very high levels.

## Comparison of risk assessment frameworks

We classified the exposure in the hydrological basins (Supplementary Fig. 1a) based on the resulting risk category for both perspectives (Fig. 4). We find that, while in the upstream perspective ~70% of total water requirements are under middle to very high risk, in the upwind perspective the number increases to 90% (Fig. 4a). As such, low upwind governance and environmental performance result in 32,900 $km^3\ yr^{-1}$ of total water requirements (75%; purple bar) under very high risk, while an upstream lack of these aspects results in much smaller freshwater requirements under very high risk (20,500 $km^3\ yr^{-1}$; 47%). This is related to the increase in the risk category of larger basins with high freshwater requirements at the expense of reductions in the categories of smaller basins with much lower water requirements. The considerably higher upwind risk is also evidenced across both GW (Fig. 4b) and BW (Fig. 4c) requirements, but most notably for the latter. These results indicate an important underestimation of transboundary water security risk emerging from upwind vulnerabilities and hazards and challenge the common practice of assessing the risk to BW requirements from changes in land and water use occurring just within the hydrological basin.

## Reassessment of global risk to water security

Notably, the upwind risk is very high in the majority of world's largest basins (Fig. 5c) owing to the large volumes of water requirements (exposure), which largely depend on the basin area ($R = 0.89$; Supplementary Table 1). Most of these large basins also exhibit high TMR dependency (Supplementary Fig. 4d) and low values of governance and environmental performance (Fig. 1 and Supplementary Fig. 6). From an upwind perspective, the Congo, Nile and Niger River basins have the largest risk to water security worldwide (Supplementary Table 2). Interestingly, these basins also have the highest risk from an upstream perspective (Supplementary Table 2). Notably, the consistent high risk among both perspectives for the Congo results from the combination of (1) high dependency on terrestrial moisture from the African continent, (2) the low governance and environmental performance of the countries located in its precipitationshed and hydrological basin, (3) the high GW requirements of its tropical vegetation and (4) its large areal extent. The Volta, Zambezi and Indus River basins are also ranked in the first ten positions of risk in both perspectives.

The differences in terms of risk from both perspectives result in a change in the ranking of hydrological basins (Figs. 5a and 6). More than half of the hydrological basins categorized with very high risk under the upstream perspective hold their risk category from an upwind perspective (Fig. 5b, 61%, top right), whereas only 38% of those in the very low risk hold their risk category (Fig. 5b, bottom left). Some of the basins with considerable changes in their risk ranking include the Amazon, Salado, Rufiji, Krishna, Yangtze and Huang He River basins, where risk increases from low (upstream) to very high (upwind) (Fig. 5a). The Amazon and Yangtze River basins, some of the largest basins on Earth, are included in the first ten risk positions from the upwind perspective, and their vulnerability increases when the TMR dependency is accounted for. For the case of the Yangtze, its precipitationshed extends over several South Asian countries with reported low governance and environmental performance (for example, India, Myanmar and Vietnam; Supplementary Fig. 2). Furthermore, it ranks high in terms of exposure (water requirements of 1,000 $km^3\ yr^{-2}$) and vulnerability (that is, many countries sharing it and ~78% of TMR).

## Discussion

Unexpected transboundary water-related risks can emerge from the interaction of upwind vulnerabilities and hazards related to governance and environmental performance. The hazards can lead to progressive land and water use changes, potentially altering the moisture supply to downwind hydrological basins[29,31,32,51,52]. Biogeophysical properties related to vegetation on land, such as those expressed by surface albedo, surface roughness length, rooting depth, leaf stomatal conductance and leaf/stem area index, control evaporation over a given

https://doi.org/10.1038/s44221-024-00291-w

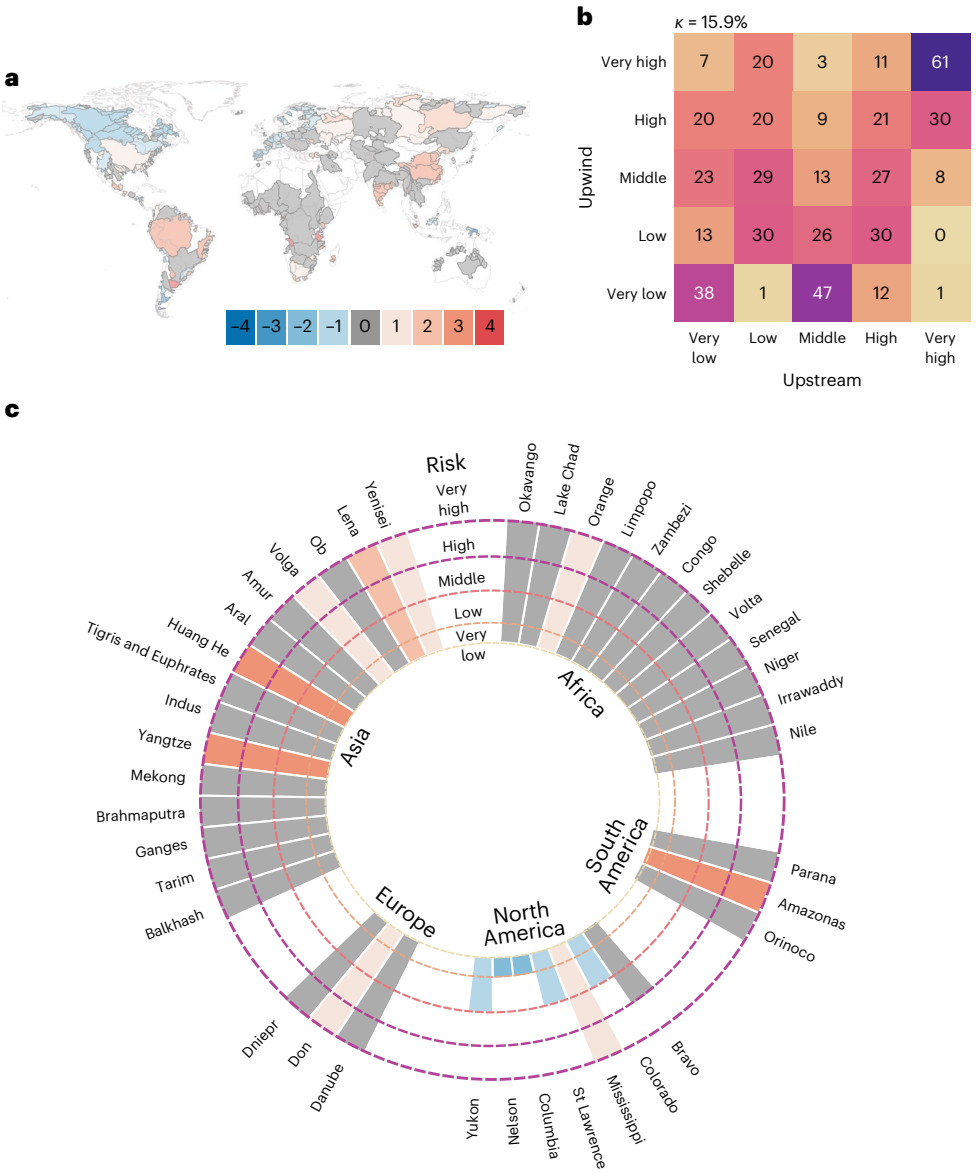


**Fig. 5 | Differences in risk categorization between perspectives. a**, Changes in risk categorization between perspectives; positive (negative) values indicate higher (lower) risk in the upwind perspective. **b**, The heat map shows the percentage agreement matrix, with the intersection between rows and columns indicating the percentage agreement of classified basins in each upwind (rows) and upstream (columns) risk category. For instance, about 11% of basins present a very high risk from an upwind perspective and a high risk from the upstream perspective. **c**, Changes in risk categorization to the 40 worldwide largest basins. The bar height indicates the risk category in the upwind perspective (see concentric circles), and its colour shows if it increases, decreases or has no changes and how many risk categories each basin changes from the upstream perspective (see colour bar in **a**).

surface. Land use changes that alter vegetation can thus drive evaporation changes, with the change magnitude and direction depending on both the original vegetation cover and that resulting after the change in land use[53–56]. For instance, the conversion of forests to grasslands mostly reduces evaporation[54,56–61]. Forest clear-cutting has been found to reduce evaporation and increase runoff; reforestation or regrowth has resulted in the opposite effect[53,55]. These changes may translate into changes in the amount of moisture advected and precipitating in downwind hydrological basins[22,23]. Hence, the degree to which this occurs depends on the type and extent of the evaporation changes and moisture convergence.

While studies[4,5,7,20,26,50,62,63] already point to the corresponding heterogeneous effects of land and water use changes on moisture supply downwind, this study rather focuses on the factors of governance and environmental performance that can impede, slow, drive or foster these changes and the corresponding risks to downwind water security. As tensions related to transboundary water governance can emerge when hydrological basins are shared by different countries or regulating authorities[64–70], tension among countries from sharing a specific precipitationshed could emerge as well. These tensions could increase when various countries are involved, requiring additional agreement and cooperation[68–70]. For instance, several basins in South America (for example, the Magdalena, Orinoco and Parana River basins) depend on moisture recycling from the Amazon Basin[7]; their precipitationsheds extend over this basin. The Amazon Basin is shared by several countries that have tried to establish agreements to reduce deforestation but with difficult progress due to each country's internal policies[34,71]. Several studies have shown the potential impacts of Amazon deforestation on precipitation and water availability in South America[7,11,18,23,50]. Accounting for upwind dependencies could then increase the interest

https://doi.org/10.1038/s44221-024-00291-w

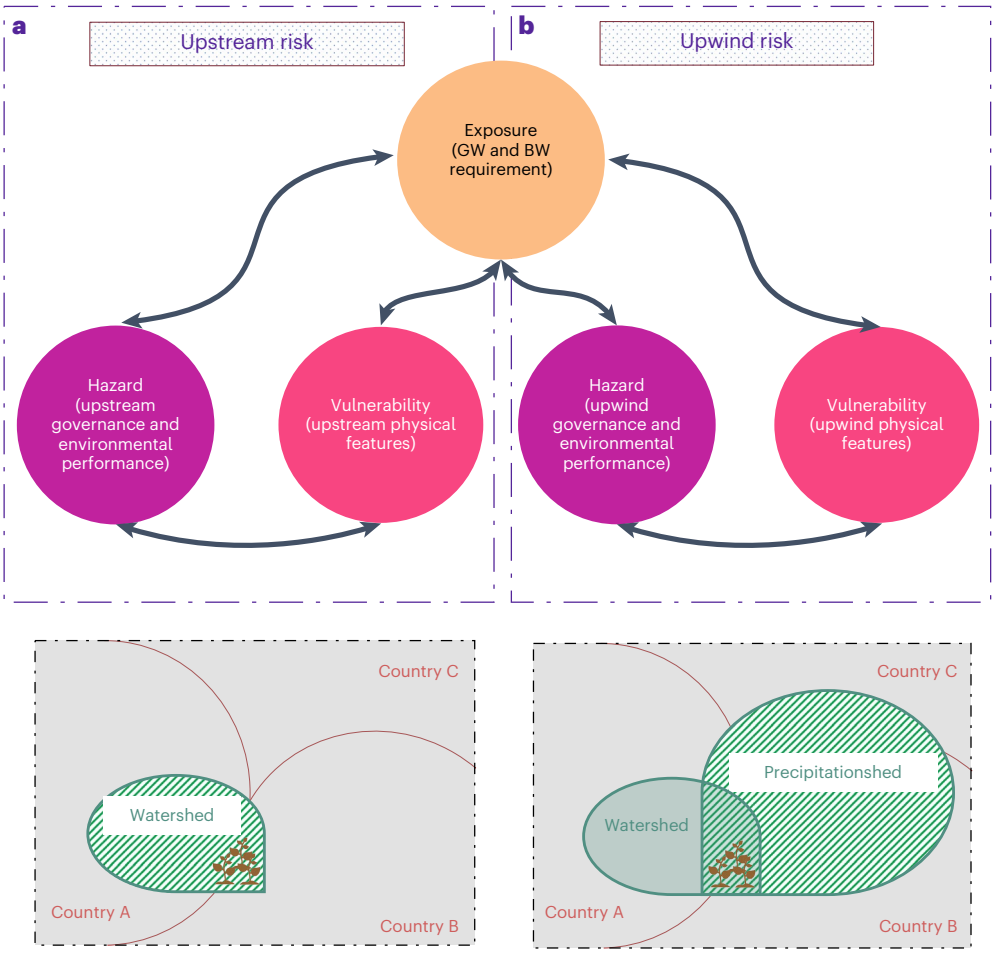


| Variable | Definition | Upstream (US) calculation | Upwind (UW) calculation |
|---|---|---|---|
| Risk | The potential consequences on a valuable subject resulting from the interaction of hazard, vulnerability and exposure within each hydrological basin and/or the precipitationshed. | $R_{US} = E_{US} \times H_{US} \times V_{US}$ | $R_{UW} = E_{UW} \times H_{UW} \times V_{UW}$ |
| Exposure | The total water requirements, determined from GW and BW volumes, for vegetation and crops within each hydrological basin. | $E_{US} = E_{UW} = GW + BW$ | |
| Hazard | Levels of governance and environmental performance of countries ($H_C$) sharing the area of a hydrological basin ($A_{ws}$) or precipitationshed ($A_{ps}$). | $H_{US} = \sum_{i=1}^{n} \frac{A_{wsi} \times H_C}{A_{ws}}$ | $H_{UW} = \sum_{i=1}^{n} \frac{A_{psi} \times H_C}{A_{ps}}$ |
| Governance | Indicator accounting for voice and accountability, political stability, government effectiveness, regulatory quality and rule of law ($G_i$) for each country. | $G = \frac{\sum_{i=1}^{n} G_i}{n}$ | |
| Environmental performance | Measure of countries' environmental management, combining 40 subindices ($EP_i$) that evaluate environmental health and ecosystem vitality across different nations. | $EP = \frac{\sum_{i=1}^{n} EP_i}{n}$ | |
| Geophysical vulnerability | The degree to which a system is susceptible to adverse effects. It depends on the system physical features. | $V_{US} = S_{US} \times F_{US} \times I_{US}$ | $V_{UW} = S_{UW} \times F_{UW} \times I_{UW} \times D_{UW}$ |
| Sensitivity | Water scarcity index (SWB) estimated as precipitation ($P$) minus evaporation ( EV) plus inter-basin surface transfers (man-made, $T$). | $S_{US} = S_{UW} = SWB = (P - EV)(1 \pm T)$ | |
| Fragility | The inverse of the hydrological basin ($A_{ws}$) or precipitationshed area ($A_{ps}$). | $F_{US} = \frac{1}{A_{ws}}$ | $F_{UW} = \frac{1}{A_{ps}}$ |
| Interdependency | Number of countries within a basin ($NC_{ws}$) or precipitationshed ($NC_{ps}$). | $I_{US} = NC_{ws}$ | $I_{UW} = NC_{ps}$ |
| TMR dependency | TMR dependency in the upwind perspective is given by the TMR ratio (TMR divided by total precipitation). | -- | $D_{UW} = \frac{TMR}{P}$ |

**Fig. 6 | Synthesis of the methodology used in this study. a**,**b**, Conceptual framework for risk assessment from upstream (**a**) and upwind (**b**) perspectives. The diagram illustrates the formulation of risk assessment approaches employed in this study, including the interaction of exposure ($E$), hazard ($H$) and vulnerability ($V$) within each hydrological basin and precipitationshed. The components of exposure (GW and BW requirements), hazard (governance and environmental performance) and vulnerability (sensitivity, fragility, interdependence and TMR dependency) are integrated to evaluate the potential consequences on water security.

in moisture upwind dependencies in the region, potentially leading to tensions between countries (understood not only as disputes between countries but also as any problem threatening regional water security) and cooperation to avoid or solve these tensions[72]. Similar issues could occur in other regions with a comparable context (for example, the Congo hydrological basin[73–75]).

Transboundary cooperation can play a crucial role in mitigating these tensions[64,68–70]. Cooperative management and agreements on shared water resources can significantly reduce tension and promote sustainable usage[28,66,68–70]. Collaborative efforts in managing surface water availability, atmospheric moisture recycling and land use changes in upwind areas are relevant for maintaining water security and preventing disputes, particularly in water-scarce regions[28,47,75,76]. This study can help detect where and to whom cooperation strategies and efforts can be addressed to mitigate the causes of water-related tensions. Nevertheless, further research is necessary to explore the mechanisms through which cooperation can be enhanced to address these challenges effectively, particularly in the face of increased demand for water resources due to climate change and the growing globalized economy[66].

Upwind risks are commonly overlooked in the assessment of transboundary water security. Moreover, not considering these risks may disregard the transboundary nature of numerous worldwide basins. The identified differences in this study, comparing a traditional upstream framework with an innovative upwind approach, reveal an underestimation of the risk to global water requirements. This emphasizes reassessing upwind transboundary basins according to their water risk levels. Such emerging results have and could lead to surprises in similar assessments for urban and energy-related water security[27,77,78]. We recommend that transboundary water security assessments add the upwind moisture dependency to the more common factors that threaten or affect water availability (for example, anthropogenic inter-basin water transfer and groundwater regional fluxes).

The co-dependence between upstream/downwind and downstream/upwind countries cannot be disregarded. For instance, again, in the case of tropical South America, large areas of the Andes are downwind of the Amazon forest, whereas most of the Amazon Basin is downstream of the Andes. Understanding this co-dependence could improve the hydro-cooperation between nations owing to the transnational mutual interests concerning water security and, hopefully, a more united approach to guarantee global long-term water security. This understanding depends on the confidence in tracking moisture simulations. Further research should be addressed to reduce uncertainty in these simulations through validation and intercomparison projects. Our findings, rather than a clear demonstration that the upwind moisture flux is threatened, is an alert showing worldwide basins where upwind risk could emerge with important implications to water security.

We invite a reflection on the common paradigm of managing and governing water beyond the hydrological basin and the required shift in assessing water-related risk and governance. The shift comprises a change from the view that uses only the concepts of hydrological basin or watershed—which have long been regarded as the best units and scales to govern and understand risks related to water changes[51,79]—to a more comprehensive view that includes atmospheric water[32]. The potential management of water beyond hydrological basin boundaries poses challenges regarding geopolitics, governance and the understanding of moisture transport. Addressing these challenges should lead to (1) the creation of new organizations or frameworks that in the future may be capable of managing water upwind or at least (2) an institutional fit of current river basin organizations to tackle the new dependencies emerging from a better understanding of moisture transport and implications for water security[80]. Assessing upwind water-related risks should improve the transboundary water agenda and help establish atmospheric governance on the water as a common good[30,31].

# Methods

## Risk assessment frameworks

We adopted the concept of risk proposed in the Intergovernmental Panel on Climate Change Sixth Assessment Report[81]. Risk is defined as the potential consequences over a valuable subject resulting from the interaction of hazard, vulnerability and exposure. Hazard is the occurrence of natural accidents or human-induced events causing harm that may adversely affect vulnerable elements, causing loss of life, injury, damage and loss to property, infrastructure, livelihoods, service provision, ecosystems and environmental resources[81]. Vulnerability is the susceptibility, propensity or predisposition to be adversely affected. Vulnerability calculations encompass a variety of concepts and elements, including sensitivity, susceptibility and resilience, among others. These elements vary according to the system being analysed and its features[82]. Exposure is the people, livelihoods, species or ecosystems, environmental functions, services, resources, infrastructure or economic, social or cultural assets that could be adversely affected[79]. Figure 6 summarizes the mathematical formulation of the risk assessment approaches employed in this study.

The traditional 'upstream' perspective analyses hazard and geophysical vulnerability within the boundaries of the hydrological basin and its surface water supply. The 'upwind perspective' focuses on hazard and geophysical vulnerability across the upwind areas contributing to the basins' moisture supply (that is, precipitationshed). Risk assessment frameworks to categorize worldwide basins according to their transboundary water security are given by equations (1) and (2):

$$R_{US} = E_{US} \times H_{US} \times V_{US} \quad (1)$$

$$R_{UW} = E_{UW} \times H_{UW} \times V_{UW}, \quad (2)$$

where $R$ is the risk, $E$ is the exposure (that is, water requirements for vegetation and crops), $H$ is the hazard and $V$ is the geophysical vulnerability. The subscripts denote the perspective used (US for upstream and UW for upwind). We now describe each risk component and any particularity related to each perspective. All risk components are categorized into five groups defined using the quantiles of the distributions across the sample of 379 hydrological basins: very high, high, middle, low and very low. We also normalized the values across the sample of the 379 transboundary basins from 0 to 1 using a min–max normalization.

## Exposure

We frame the exposed asset of the risk assessment as the total water requirements for vegetation and crops, which are determined from the long-term annual requirements of GW and BW volumes for vegetation and crops within each hydrological basin. The exposure is the same for both upstream ($E_{US}$) and upwind perspectives ($E_{UW}$), relating to water requirements within the basin (equation (3)).

$$E_{US} = E_{UW} = GW + BW \quad (3)$$

GW is defined as the fraction of precipitation that infiltrates into the soil and is then evaporated or transpired by vegetation and crops. BW is the freshwater in surface and groundwater resource usually provided to vegetation or crops through irrigation and then evaporated or transpired. Estimations of GW and BW are obtained from a global gridded (5 arcminute) dataset of annual green and blue long-term water requirements of all land covers, natural and anthropogenic, existing within each hydrological basin during the analysis period (2008–2017). Agricultural land covers present 23 types of crop and three crop groups from the Global Spatially-Disaggregated Crop Production Statistics Data (also known as Spatial Production Allocation Mode, or SPAM) for 2010. These estimations were performed using the WATNEEDS model[83], assessing the vertical component of the soil water balance, computing

evaporation on each watershed area unit of the hydrological basin with the Penman–Monteith method[84] as modified by Allen et al.[85]. Overland flow is calculated as a soil water saturation excess mechanism and percolation is a linear function of the maximum infiltration rate and soil moisture. For a detailed description of the WATNEEDS model, we refer the reader to Chiarelli et al.[83]. Data used to calculate water requirements are reported in Table 1.

**Table 1 | Data used to calculate water needs**

| Climate data | Data source |
|---|---|
| Precipitation | CRU CL 2.0[106] |
| Reference evaporation | CRU CL 2.0[106] |
| **Soil water data** | **Data source** |
| Maximum water content available in the soil | HWSD, FAO[107] |
| Maximum infiltration rate | BGR and UNESCO[108] |
| **Crop parameters** | **Data source** |
| Sowing date | MIRCA2000[109] |
| Crop constant (kc) | Siebert et al.[110] |
| Growth stages | Siebert et al.[110] |
| **Crop data** | **Data source** |
| Cultivated area, yield | Yu et al.[111] |

## Hazard

Although the Intergovernmental Panel on Climate Change commonly uses the term hazard for climate-related physical events, trends or their physical impacts[81], we here focus on potential human-induced hazards related to levels of governance and environmental performance. For human-induced hazards, features related to societal issues indicate the type of activity that may threaten a given system. A thorough threat assessment requires collecting information on potential threat activities within each country. Traditionally, relevant public indices have been used for this[86]. We calculated long-term hazard ($H_C$) during 2008–2017 at a country scale emerging from low levels of governance ($G$) and environmental performance (EP) as (equation (4) and Supplementary Fig. 2)

$$H_C = G^{-1} \times \mathrm{EP}^{-1}. \quad (4)$$

For this, we used the five World Bank's Governance subindices for each country ($G_i$) reported during 2008–2017[87], addressing fundamental aspects of governance: (1) voice and accountability, examining the degree of civil society involvement in governmental processes, (2) political stability, focusing on the likelihood of political instability and violence, (3) government effectiveness, evaluating the government's capacity to implement policies and provide services efficiently, (4) regulatory quality, highlighting the transparency and effectiveness of regulatory frameworks, and (5) rule of law, measuring the fair and equitable application of laws. We used the long-term average of these subindices to estimate each country's level of governance (equation (5)), where $n$ is the number of years.

$$G = \frac{\sum_{i=1}^{n} G_i}{n} \quad (5)$$

In summary, voice and accountability measure political, civil and human rights and relate to the level of participation in selecting government and the freedom of expression, association and free media[87]. A decrease in voice and accountability can, for instance, disregard the call from citizens to control or curve environmental degradation that may lead to modifications of vapour flows travelling downwind by activities such as deforestation.

Political stability measures the likelihood of violent threats to, or changes in, government, including terrorism, and can relate to the level of bellicosity of a government to generate changes that may affect the moisture supply downstream or downwind. For instance, low political instability would hamper the control of illegal practices fuelling environmental degradation, such as illicit agricultural expansion and mining.

Government effectiveness visualizes the competence of the bureaucracy and the quality of public service delivery, and a low value would imply a limited capacity of the government to control environmental degradation per se. Regulatory quality measures the incidence of policies that are unfriendly to markets. It also refers to a country's internationalization level and immersion in the international agenda by international commitments and regulations.

Regulatory quality would directly target the issues related to shared political institutions (such as international political and legal arrangements). It also represents the complexity of political frameworks considering different levels of organization (scales), for example, multiple countries (for example, the European Union), or inside countries (there are also problems inside countries, for example, among states sharing the Colorado River in the USA). Hence, a low regulatory quality will imply a higher water security hazard.

Rule of law shows the measuring perceptions of the extent to which agents have confidence in and abide by the rules of society, mostly concerning the quality of contract enforcement, the police and the courts and the likelihood of crime and violence. A low score of rule and law increases the hazard of water security. Finally, the control of corruption, which measures corruption and state capture, also relates to the potential of controlling and avoiding environmental degradation. A low score also implies a higher hazard of water security.

These subindices are combined to offer a holistic view of governance in each country, enabling meaningful comparisons on a global scale. Furthermore, we used the 40 subindices of the Environmental Performance Index by the Yale Center for Environmental Law and Policy[88]. This comprehensive measure of the countries' environmental management evaluates environmental health and ecosystem vitality across different nations. The index considers indicators such as water resources management, biodiversity conservation and climate change mitigation efforts. Some of these subindices are pertinent for the upstream and upwind risks to water security, as they relate directly to land use changes that may potentially affect downwind moisture supply. These include tree cover loss, grassland loss, wetland loss and terrestrial biome protection. By analysing these factors, the index provides insights into a country's environmental policies, their effectiveness and areas for improvement. This index is valuable for policymakers and researchers to assess progress and prioritize actions towards sustainable development and environmental protection globally. We know that several subindices of the environmental performance metric are not related to water and land cover environmental characteristics. However, we prefer to use the full metric as a holistic proxy of environmental performance relevant to water security rather than arbitrarily selecting and dropping specific subindices. Thus, we calculated the environmental performance as the long-term average of these 40 subindices ($\mathrm{EP}_i$) (equation (6)), where $n$ is the number of years.

$$\mathrm{EP} = \frac{\sum_{i=1}^{n} \mathrm{EP}_i}{n} \quad (6)$$

Upstream hazard was calculated for each hydrological basin as an area-weighted average for all countries within the hydrological basin ($H_{US}$; equation (7)). Upwind hazard ($H_{UW}$) was calculated similarly but using the precipitationshed area instead of the hydrological basin area

(equation (8)). The $n$ is the number of countries sharing the basin or precipitationshed.

$$H_{US} = \sum_{i=1}^{n} \frac{A_{ws_i} \times H_C}{A_{ws}} \quad (7)$$

$$H_{UW} = \sum_{i=1}^{n} \frac{A_{ps_i} \times H_C}{A_{ps}} \quad (8)$$

Here $A_{ws}$ and $A_{ps}$ represent the areas for each ($i$) of the total countries ($n$) falling in the hydrological basin and precipitationshed, respectively.

### Geophysical vulnerability

Vulnerability is a physical feature used for quantifying risk[76]. This study calculated geophysical vulnerability ($V$) as a function of different physical variables, which sometimes differed between both perspectives. From an upstream perspective (equation (9)), vulnerability is a function of hydrological basin features: sensitivity ($S$), fragility ($F$) and interdependency ($I$). From an upwind perspective (equation (10)), we added one more variable related to TMR dependency ($D$). Fragility and interdependency were adjusted to the spatial extent of the precipitationshed to represent the physical links established by upwind moisture dependency. Again, subscripts denote the perspective used (US, upstream; UW, upwind).

$$V_{US} = S_{US} \times F_{US} \times I_{US} \quad (9)$$

$$V_{UW} = S_{UW} \times F_{UW} \times I_{UW} \times D_{UW} \quad (10)$$

### Sensitivity

Sensitivity is calculated from a min–max normalized water scarcity index estimated as precipitation ($P$) minus actual evaporation (EV) plus inter-basin surface transfers (man-made, $T$). Precipitation and actual evaporation are based on data from ERA5 from 2008 to 2017, which estimate the long-term mean of surface water balance (SWB)[89]. For inter-basin surface transfers, we have gathered data on transfers from several references, most importantly from Dynesius and Nilsson[90], who document inter-basin transfers in 139 hydrological basins worldwide. They report the amount of freshwater transferred as a percentage of the runoff before any manipulation. The data even specify if the effect of the inter-basin transfer is negative or positive. Hence, we adjust the values of $P$ − EV originally obtained from ERA5 data with this estimate accordingly. For other basins not included in the work of Dynesius and Nilsson[90], we have also relied on different sources mentioned in the global assessment of Nilsson et al.[91] and other sources such as Dobbs et al.[92] and Gupta and van der Zaag[93]. Note that the data on inter-basin transfers may not agree with the ERA5 data, yet we have to assume that the amount of water transferred is constant in time and that some inter-basin transfers may not be reported in these databases.

We used the same sensitivity estimate for both perspectives (equation (11)). To homogenize the values across the sample of the 379 transboundary basins, all $N$ values were normalized from 0 to 1 (equations (12) and (13)) using the maximum ($SWB_{MAX}$) and minimum ($SWB_{MIN}$) values of the sample. We inverted the value so that higher values represent more sensitivity to upwind or upstream changes in water availability due to less water running on the hydrological basin's surface, which agrees with higher risk corresponding to higher sensitivity. We assume that the water requirements are less vulnerable to governance and environmental performance changes when more water is available in the hydrological basin.

$$SWB = (P - EV)(1 \pm T) \quad (11)$$

$$SWB_N = (SWB - SWB_{MIN})/(SWB_{MAX} - SWB_{MIN}) \quad (12)$$

$$S_{US} = S_{UW} = 1 - SWB_N \quad (13)$$

### Fragility

From the upstream perspective (equation (14)), fragility relates to the inverse of the area of the hydrological basin ($A_{ws}$), while from an upwind standpoint (equation (15)), it relates to that of the precipitationshed ($A_{ps}$) (Supplementary Fig. 5). To homogenize the values across the sample of the 379 transboundary basins, all values were normalized from 0 to 1. From the first perspective, we assume that the socioecological system and capacity to meet the freshwater requirements within the hydrological basin is more fragile to changes in governance and environmental performance in smaller hydrological basins than in large basins. For instance, in a larger basin, it is most likely that, while some freshwater requirements are affected in some parts of the hydrological basin, other parts will not experience such affectation. On the contrary, in a small hydrological basin, all freshwater requirements will most possibly be affected similarly[52,94]. In the upwind perspective, a similar logic is proposed: the freshwater requirements in a hydrological basin will be less affected when the basin has a large precipitationshed, as the particular hazard in an upwind country may not be as representative when other countries and land areas are involved.

$$F_{US} = \frac{1}{A_{ws}} \quad (14)$$

$$F_{UW} = \frac{1}{A_{ps}} \quad (15)$$

### Interdependency

From the upstream perspective (equation (16)), interdependency is estimated from the number of countries within a basin ($NC_{ws}$). From the upwind perspective (equation (17)), this variable depends on the countries sharing the precipitationshed ($NC_{ps}$). For both perspectives, high values represent a high interdependency with cooperation concerning water resources more difficult between several countries[95]. The assumption is that it will be easier to establish management measures and cooperation if the number of countries is lower. We must state that the level of cooperation in water governance does not strictly depend on the number of countries but also on other factors related to governance, which, for this particular assessment, we include as part of the hazard (see 'Hazard' section). To homogenize the values across the sample of the 379 transboundary basins, all values were normalized from 0 to 1.

$$I_{US} = NC_{ws} \quad (16)$$

$$I_{UW} = NC_{ps} \quad (17)$$

### TMR dependency

The TMR dependency in the upwind perspective (Duw; equation (18)) relates to the contribution of continental evaporation to precipitration in the hydrological basin (Pc). The higher the value, the higher the dependency on TMR.

$$D_{UW} = \frac{Pc}{P} \quad (18)$$

Finally, we explored collinearity between all variables involved in the risk assessment. As a summary, we found that the variables involved in calculating risk show low collinearity in both perspectives (Supplementary Tables 3 and 4), indicating that risk results from nonlinear interactions between its components. Upstream interdependency

(that is, the number of countries upstream) correlates highly with upstream risk (Supplementary Table 1). From the upwind perspective, we found a high correlation between interdependency and vulnerability (Supplementary Table 5).

### Characterizing TMR ratio in worldwide basins

We used the vectorized polygon dataset from the Major River Basins of the World project of the Global Runoff Data Centre to extract the large hydrological basins used in our risk assessments[96]. This dataset incorporates data from the HydroSHEDS database[97] and provides the boundaries of 405 river basins. A total of 26 of these basins are not transboundary from the viewpoint of neither the upwind nor the upstream perspectives.

We quantified the TMR ratio in all basins on the basis of the tracking simulation performed by Tuinenburg et al.[74] using the UTrack model[98] at 1.0° resolution (available at https://doi.pangaea.de/10.1594/PANGAEA.912710). This simulation spans from 2008 to 2017 and presents monthly climatological means for recycling. Correspondingly, we use this period as the reference for our risk assessments. The UTrack is a Lagrangian moisture tracking numerical algorithm used to study worldwide atmospheric moisture transport processes[99–103]. The model tracks parcels of moisture through the atmosphere from their evaporation sources to precipitation sinks. First, evaporated moisture from the land surface is released into atmospheric parcels. Next, atmospheric trajectories for each parcel are calculated, and finally, the moisture contribution to precipitation in each grid cell for each parcel is allocated. For a further detailed description of the UTrack, refer to Tuinenburg and Staal[98]. Calculations of TMR ratio (that is, precipitation fraction with terrestrial origin) used data of precipitation, precipitable water, evaporation, wind speed and direction obtained from the ERA5 reanalysis on a 0.25° global grid.

To obtain the TMR ratio of a hydrological basin, we took all evaporation contribution fractions from the continental sources towards each basin and multiplied them with evaporation to estimate the moisture flow. Finally, we summed these fluxes and divided them by the total precipitation over the basin. Finally, for validation and assessing uncertainty, we compared for specific hydrological basins the TMR dependency results obtained with UTrack with those obtained with simulations using the Eulerian WAM2-Layers model[104] (see Supplementary Fig. 7 and the 'Uncertainty analysis' section).

### Structuring the transboundary precipitationshed

Keys et al.[20] define a precipitationshed as the upwind surface areas providing evaporation as a contribution to precipitation in a determined location. The precipitationshed is then calculated using polygons to delimit regions according to contribution levels. Previous studies have suggested and discussed different thresholds to delimit a precipitationshed boundary of continental recycled precipitation (for example, 70% (ref. 20) and 40% (ref. 50)). We here used a higher value (80%) based on (1) an uncertainty exploration (Supplementary Fig. 7b,c), (2) the moisture tracking state of the art (it is higher than the minimum required to delineate our precipitationsheds[50]) and (3) the need for high representativeness of continental sources.

We used the UTrack dataset to delimit the transboundary precipitationshed for each hydrological basin. First, we took evaporation contribution fluxes from the continental sources towards each basin; next, we divided these values by each basin's total precipitation to obtain the continental precipitation recycling ratio per pixel. Finally, we used these values to delimit the regions according to contribution levels. Following Weng et al.[50], we used the terrestrial component of precipitationsheds in our calculations because land surface alterations in each country could directly impact the TMR. The estimation of TMR and precipitationshed extent from the UTrack dataset is justified by the lower computational costs compared with those when performing a tracking simulation. Furthermore, the UTrack simulation that generates this dataset uses the ERA5 data with a 0.25° high-resolution climatological dataset. We explored the uncertainty in our estimates of precipitationsheds' extensions by comparing those from the ten largest worldwide basins using WAM2-Layers (Supplementary Fig. 7b,c).

### Uncertainty analysis

We studied uncertainty in our results related to the hazard and the physical links introduced by upwind dependencies. First, we analysed the sensitivity of the results regarding the risk arising from different governance and environmental performance values by using twice the standard deviations of all their subindices during 2008–2017, generating a range of possible results (Supplementary Fig. 8).

Furthermore, uncertainty from tracking moisture simulations arises because these models use a simplified representation of the real-world and climatological data. To explore these uncertainties, we compared the estimated TMR dependency and precipitationshed from the UTrack dataset with simulations using WAM2-Layers in the ten largest basins worldwide. These models present different physical approaches (Lagrangian versus Eulerian) and climatological inputs (ERA5 versus ERA-Interim, with 0.25° and 1.5° of spatial resolution, respectively). This comparison was constrained to a few hydrological basins owing to the high computational costs of using WAM2-Layers to estimate the extension of precipitationsheds. Unfortunately, the previous tracking simulation dataset using this model[104] does not allow us to estimate the extension of the precipitationshed. For further details on the uncertainty analysis, see Supplementary Information.

## Data availability

Data results are available via Zenodo at https://doi.org/10.5281/zenodo.11474249 (ref. 105) with CCA 4.0 licence.

## Code availability

Code used to delimit continental precipitationsheds from UTrack dataset is available via GitHub at https://github.com/josepomarin/PshedUTrack.git.

## References

1. van der Ent, R. J., Savenije, H. H. G., Schaefli, B. & Steele-Dunne, S. C. Origin and fate of atmospheric moisture over continents. *Water Resour. Res.* **46**, 1–12 (2010).
2. van der Ent, R. J., Wang-Erlandsson, L., Keys, P. W. & Savenije, H. H. G. Contrasting roles of interception and transpiration in the hydrological cycle—part 2: moisture recycling. *Earth Syst. Dynam.* **5**, 471–489 (2014).
3. Gordon, L. J. et al. Human modification of global water vapor flows from the land surface. *Proc. Natl Acad. Sci. USA* **102**, 7612–7617 (2005).
4. Wang-Erlandsson, L. et al. Remote land use impacts on river flows through atmospheric teleconnections. *Hydrol. Earth Syst. Sci.* **22**, 4311–4328 (2018).
5. te Wierik, S. A., Cammeraat, E. L. H., Gupta, J. & Artzy-Randrup, Y. A. Reviewing the impact of land use and land-use change on moisture recycling and precipitation patterns. *Water Resour. Res.* **57**, e2020WR029234 (2021).
6. Destouni, G., Jaramillo, F. & Prieto, C. Hydroclimatic shifts driven by human water use for food and energy production. *Nat. Clim. Change* **3**, 213–217 (2013).
7. Ruiz-Vásquez, M., Arias, P. A., Martínez, J. A. & Espinoza, J. C. Effects of Amazon basin deforestation on regional atmospheric circulation and water vapor transport towards tropical South America. *Clim. Dyn.* **54**, 4169–4189 (2020).
8. Jaramillo, F. & Destouni, G. Local flow regulation and irrigation raise global human water consumption and footprint. *Science* **350**, 1248–1251 (2015).

9. Creed, I. F. et al. Changing forest water yields in response to climate warming: results from long-term experimental watershed sites across North America. *Global Change Biol.* **20**, 3191–3208 (2014).
10. Hegerl, G. C. et al. Challenges in quantifying changes in the global water cycle. *Bull. Am. Meteorol. Soc.* **96**, 1097–1115 (2015).
11. Badger, A. M. & Dirmeyer, P. A. Climate response to Amazon forest replacement by heterogeneous crop cover. *Hydrol. Earth Syst. Sci.* **19**, 4547–4557 (2015).
12. Bagley, J. E., Desai, A. R., Dirmeyer, P. A. & Foley, J. A. Effects of land cover change on moisture availability and potential crop yield in the worlds breadbaskets. *Environ. Res. Lett.* **7**, 014009 (2012).
13. Dirmeyer, P. A. & Brubaker, K. L. Contrasting evaporative moisture sources during the drought of 1988 and the flood of 1993. *J. Geophys. Res. Atmos.* **104**, 19383–19397 (1999).
14. Dominguez, F., Kumar, P., Liang, X.-Z. & Ting, M. Impact of atmospheric moisture storage on precipitation recycling. *J. Clim.* **19**, 1513–1530 (2006).
15. Keys, P. W., Wang-Erlandsson, L. & Gordon, L. J. Revealing invisible water: moisture recycling as an ecosystem service. *PLoS ONE* **11**, e0151993 (2016).
16. Lo, M.-H. & Famiglietti, J. S. Irrigation in California's Central Valley strengthens the southwestern U.S. water cycle. *Geophys. Res. Lett.* **40**, 301–306 (2013).
17. Salih, A. A. M., Körnich, H. & Tjernström, M. Climate impact of deforestation over South Sudan in a regional climate model. *Int. J. Climatol.* **33**, 2362–2375 (2013).
18. Swann, A. L. S., Longo, M., Knox, R. G., Lee, E. & Moorcroft, P. R. Future deforestation in the Amazon and consequences for South American climate. *Agric. For. Meteorol.* **214–215**, 12–24 (2015).
19. Keune, J., Sulis, M., Kollet, S., Siebert, S. & Wada, Y. Human water use impacts on the strength of the continental sink for atmospheric water. *Geophys. Res. Lett.* **45**, 4068–4076 (2018).
20. Keys, P. W. et al. Analyzing precipitationsheds to understand the vulnerability of rainfall dependent regions. *Biogeosciences* **9**, 733–746 (2012).
21. Piemontese, L. et al. Estimating the global potential of water harvesting from successful case studies. *Global Environ. Change* **63**, 102121 (2020).
22. Lawrence, D. & Vandecar, K. Effects of tropical deforestation on climate and agriculture. *Nat. Clim. Change* **5**, 27–36 (2015).
23. Stickler, C. M. et al. Dependence of hydropower energy generation on forests in the Amazon Basin at local and regional scales. *Proc. Natl Acad. Sci. USA* **110**, 9601–9606 (2013).
24. Li, D., Wu, S., Liu, L., Zhang, Y. & Li, S. Vulnerability of the global terrestrial ecosystems to climate change. *Global Change Biol.* **24**, 4095–4106 (2018).
25. Côté, I. M. & Darling, E. S. Rethinking ecosystem resilience in the face of climate change. *PLoS Biol.* **8**, e1000438 (2010).
26. Fahrländer, S. F., Wang-Erlandsson, L., Jaramillo, F. & Pranindita, A. Hydroclimatic vulnerability of wetlands to upwind land use changes. *Earth's Future* **12**, e2023EF003837 (2024).
27. Keys, P. W., Wang-Erlandsson, L. & Gordon, L. J. Megacity precipitationsheds reveal tele-connected water security challenges. *PLoS ONE* **13**, e0194311 (2018).
28. Keys, P. W., Wang-Erlandsson, L., Gordon, L. J., Galaz, V. & Ebbesson, J. Approaching moisture recycling governance. *Global Environ. Change* **45**, 15–23 (2017).
29. Posada-Marín, J. A. & Salazar, J. F. River flow response to deforestation: contrasting results from different models. *Water Security* **15**, 100115 (2022).
30. Ahlström, H. et al. An earth system law perspective on governing social-hydrological systems in the Anthropocene. *Earth Syst. Govern.* **10**, 100120 (2021).
31. Rockström, J., Mazzucato, M., Andersen, L. S., Fahrländer, S. F. & Gerten, D. Why we need a new economics of water as a common good. *Nature* **615**, 794–797 (2023).
32. Keune, J. & Miralles, D. G. A precipitation recycling network to assess freshwater vulnerability: challenging the watershed convention. *Water Resour. Res.* **55**, 9947–9961 (2019).
33. te Wierik, S. A., Gupta, J., Cammeraat, E. L. H. & Artzy-Randrup, Y. A. The need for green and atmospheric water governance. *WIREs Water* **7**, e1406 (2020).
34. Salazar, A. et al. Peace and the environment at the crossroads: elections in a conflict-troubled biodiversity hotspot. *Environ. Sci. Policy* **135**, 77–85 (2022).
35. Fischer, R., Giessen, L. & Günter, S. Governance effects on deforestation in the tropics: a review of the evidence. *Environ. Sci. Policy* **105**, 84–101 (2020).
36. Larson, A. M., Sarmiento Barletti, J. P. & Heise Vigil, N. A place at the table is not enough: accountability for Indigenous Peoples and local communities in multi-stakeholder platforms. *World Dev.* **155**, 105907 (2022).
37. United Nations Secretary-General. *71st Report of the Open-ended Intergovernmental Expert Working Group on Indicators and Terminology relating to Disaster Risk Reduction* (UNDRR, 2017).
38. Vörösmarty, C. J. et al. Global threats to human water security and river biodiversity. *Nature* **467**, 555–561 (2010).
39. Hall, J. & Borgomeo, E. Risk-based principles for defining and managing water security. *Philos. Trans. R. Soc. A* **371**, 20120407 (2013).
40. Garrick, D. & Hall, J. W. Water security and society: risks, metrics, and pathways. *Annu. Rev. Environ. Resour.* **39**, 611–639 (2014).
41. Shi, R., Wang, T., Yang, D. & Yang, Y. Streamflow decline threatens water security in the upper Yangtze river. *J. Hydrol.* **606**, 127448 (2022).
42. Drenkhan, F. et al. Looking beyond glaciers to understand mountain water security. *Nat. Sustain.* **6**, 130–138 (2023).
43. Sobhani, P. et al. Assessing water security and footprint in hypersaline Lake Urmia. *Ecol. Indic.* **155**, 110955 (2023).
44. Bergier, I. et al. Amazon rainforest modulation of water security in the Pantanal wetland. *Sci. Total Environ.* **619–620**, 1116–1125 (2018).
45. Castle, S. L. et al. Groundwater depletion during drought threatens future water security of the Colorado River Basin. *Geophys. Res. Lett.* **41**, 5904–5911 (2014).
46. Chawla, I., Karthikeyan, L. & Mishra, A. K. A review of remote sensing applications for water security: quantity, quality, and extremes. *J. Hydrol.* **585**, 124826 (2020).
47. Rijsberman, F. R. Water scarcity: fact or fiction? *Agric. Water Manage.* **80**, 5–22 (2006).
48. Hanemann, W. M. The economic conception of water. in *Water Crisis: Myth or Reality?* (eds Rogers, P. P., Llamas, M. R. & Martinez-Cortina, L.) 61–91 (Taylor & Francis, 2006).
49. Loomis, R. A. Y. & John, B. *Determining the Economic Value of Water: Concepts and Methods* (Routledge, 2014).
50. Weng, W., Luedeke, M., Zemp, D., Lakes, T. & Kropp, J. Aerial and surface rivers: downwind impacts on water availability from land use changes in Amazonia. *Hydrol. Earth Syst. Sci.* **22**, 911–927 (2018).
51. Cohen, A. Rescaling environmental governance: watersheds as boundary objects at the intersection of science, neoliberalism, and participation. *Environ. Plan A* **44**, 2207–2224 (2012).
52. Coe, M. T., Costa, M. H. & Soares-Filho, B. S. The influence of historical and potential future deforestation on the stream flow of the Amazon River–Land surface processes and atmospheric feedbacks. *J. Hydrol.* **369**, 165–174 (2009).
53. Sørensen, R. et al. Forest harvest increases runoff most during low flows in two boreal streams. *Ambio* **38**, 357–363 (2009).

54. Loarie, S. R., Lobell, D. B., Asner, G. P., Mu, Q. & Field, C. B. Direct impacts on local climate of sugar-cane expansion in Brazil. *Nat. Clim. Change* **1**, 105–109 (2011).
55. Qiu, G. Y., Xie, F., Feng, Y. C. & Tian, F. Experimental studies on the effects of the 'Conversion of Cropland to Grassland Program' on the water budget and evapotranspiration in a semi-arid steppe in Inner Mongolia, China. *J. Hydrol.* **411**, 120–129 (2011).
56. Sterling, S. M., Ducharne, A. & Polcher, J. The impact of global land-cover change on the terrestrial water cycle. *Nat. Clim. Change* **3**, 385–390 (2013).
57. Bosch, J. M. & Hewlett, J. D. A review of catchment experiments to determine the effect of vegetation changes on water yield and evapotranspiration. *J. Hydrol.* **55**, 3–23 (1982).
58. Martin, P., Rosenberg, N. J. & McKenney, M. S. Sensitivity of evapotranspiration in a wheat field, a forest, and a grassland to changes in climate and direct effects of carbon dioxide. *Clim. Change* **14**, 117–151 (1989).
59. Costa, M. H. & Foley, J. A. Combined effects of deforestation and doubled atmospheric $CO_2$ concentrations on the climate of Amazonia. *J. Clim.* **13**, 18–34 (2000).
60. Andréassian, V. Waters and forests: from historical controversy to scientific debate. *J. Hydrol.* **291**, 1–27 (2004).
61. Ellison, D., N. Futter, M. & Bishop, K. On the forest cover–water yield debate: from demand- to supply-side thinking. *Global Change Biol.* **18**, 806–820 (2012).
62. D'Almeida, C. et al. The effects of deforestation on the hydrological cycle in Amazonia: a review on scale and resolution. *Int. J. Climatol.* **27**, 633–647 (2007).
63. Sierra, J. P. et al. Deforestation impacts on Amazon-Andes hydroclimatic connectivity. *Clim. Dynam.* **58**, 2609–2636 (2022).
64. Wolf, A. T. A long-term view of water and security: international waters, national issues and regional tensions. *J Contemp. Wat. Res. Ed.* **142**, 67–75 (2009).
65. Nasr, H. & Neef, A. Ethiopia's challenge to Egyptian hegemony in the Nile River Basin: the case of the grand Ethiopian Renaissance Dam. *Geopolitics* **21**, 969–989 (2016).
66. Petersen-Perlman, J. D., Veilleux, J. C. & Wolf, A. T. International water conflict and cooperation: challenges and opportunities. *Water Int.* **42**, 105–120 (2017).
67. Elsayed, H., Djordjević, S., Savić, D. A., Tsoukalas, I. & Makropoulos, C. The Nile water–food–energy nexus under uncertainty: impacts of the Grand Ethiopian Renaissance Dam. *J. Water Resour. Plan. Manage.* **146**, 04020085 (2020).
68. Wolf, A. T. Transboundary water conflicts and cooperation. in *Allocating and Managing Water for a Sustainable Future: Lessons from Around the World (Summer Conference, June 11–14)* (2002).
69. Rai, S. P., Wolf, A. T., Sharma, N., & Tiwari, H. Hydropolitics in transboundary water conflict and cooperation. in *River System Analysis and Management* (ed. Sharma, N.) 353–368 (Springer Singapore, 2017).
70. Turgul, A. et al. Reflections on transboundary water conflict and cooperation trends. *Water Int.* **49**, 274–288 (2024).
71. Pereira, E. J. D. A. L., de Santana Ribeiro, L. C., da Silva Freitas, L. F. & de Barros Pereira, H. B. Brazilian policy and agribusiness damage the Amazon rainforest. *Land Use Policy* **92**, 104491 (2020).
72. Levy, B. S. & Sidel, V. W. Water rights and water fights: preventing and resolving conflicts before they boil over. *Am. J. Public Health* **101**, 778–780 (2011).
73. Butsic, V., Baumann, M., Shortland, A., Walker, S. & Kuemmerle, T. Conservation and conflict in the Democratic Republic of Congo: the impacts of warfare, mining, and protected areas on deforestation. *Biol. Conserv.* **191**, 266–273 (2015).
74. Tuinenburg, O. A., Theeuwen, J. J. & Staal, A. High-resolution global atmospheric moisture connections from evaporation to precipitation. *Earth Syst. Sci. Data* **12**, 3177–3188 (2020).
75. Nyasulu, M. K. et al. African rainforest moisture contribution to continental agricultural water consumption. *Agric. For. Meteorol.* **346**, 109867 (2024).
76. Gain, A. K. & Giupponi, C. A dynamic assessment of water scarcity risk in the Lower Brahmaputra River Basin: an integrated approach. *Ecol. Indic.* **48**, 120–131 (2015).
77. Krueger, E. H. et al. Resilience dynamics of urban water supply security and potential of tipping points. *Earth's Future* **7**, 1167–1191 (2019).
78. D'Odorico, P. et al. The global food–energy–water nexus. *Rev. Geophys.* **56**, 456–531 (2018).
79. Abbott, B. W. et al. Human domination of the global water cycle absent from depictions and perceptions. *Nat. Geosci.* **12**, 533–540 (2019).
80. Moore, M.-L. et al. Moving from fit to fitness for governing water in the Anthropocene. *Nat Water* **2**, 511–520 (2024).
81. Reisinger, A. et al. The concept of risk in the IPCC Sixth Assessment Report: a summary of cross-working group discussions. *IPCC* https://www.ipcc.ch/site/assets/ (2020).
82. Estoque, R. C. et al. Has the IPCC's revised vulnerability concept been well adopted? *Ambio* **52**, 376–389 (2023).
83. Chiarelli, D. D. et al. The green and blue crop water requirement WATNEEDS model and its global gridded outputs. *Sci. Data* **7**, 273 (2020).
84. Harris, I., Jones, P. D., Osborn, T. J. & Lister, D. H. Updated high-resolution grids of monthly climatic observations—the CRU TS3.10 dataset. *Int. J. Climatol.* **34**, 623–642 (2014).
85. Allan, R. G., Pereira, L. S., Raes, D. & Smith, M. *Crop Evapotranspiration—Guidelines for Computing Crop Water Requirements* (FAO, 1998).
86. Caldara, D. & Lacoviello, M. Measuring geopolitical risk. *Am. Econ. Rev.* **112**, 1194–1225 (2022).
87. Kaufmann, D. & Kraay, A. Governance indicators: where are we, where should we be going? *World Bank Res. Observ.* **23**, 1–30 (2008).
88. Hsu, A., & Zomer, A. Environmental performance index. in *Wiley StatsRef: Statistics Reference Online* (John Wiley & Sons, 2014).
89. Schyns, J. F., Hoekstra, A. Y. & Booij, M. J. Review and classification of indicators of green water availability and scarcity. *Hydrol. Earth Syst. Sci.* **19**, 4581–4608 (2015).
90. Dynesius, M. & Nilsson, C. Fragmentation and flow regulation of river systems in the northern third of the world. *Science* **266**, 753–762 (1994).
91. Nilsson, C., Reidy, C. A., Dynesius, M. & Revenga, C. Fragmentation and flow regulation of the world's large river systems. *Science* **308**, 405–408 (2005).
92. Dobbs, G. R. et al. Inter-basin surface water transfers database for public water supplies in conterminous United States, 1986–2015. *Sci. Data* **10**, 255 (2023).
93. Gupta, J. & van der Zaag, P. Interbasin water transfers and integrated water resources management: where engineering, science and politics interlock. *Phys. Chem. Earth Parts A/B/C* **33**, 28–40 (2008).
94. Salazar, J. F. et al. Scaling properties reveal regulation of river flows in the Amazon through a 'forest reservoir.'. *Hydrol. Earth Syst. Sci.* **22**, 1735–1748 (2018).
95. Villar, P. C., Ribeiro, W. C. & Sant'Anna, F. M. Transboundary governance in the La Plata River basin: status and prospects. *Water Int.* **43**, 978–995 (2018).
96. *Major River Basins of the World/Global Runoff Data Centre* (Global Runoff Data Centre (GRDC), 2020).
97. Lehner, B. & Grill, G. Global river hydrography and network routing: baseline data and new approaches to study the world's large river systems. *Hydrol. Process.* **27**, 2171–2186 (2013).

98. Tuinenburg, O. A. & Staal, A. Tracking the global flows of atmospheric moisture and associated uncertainties. *Hydrol. Earth Syst. Sci.* **24**, 2419–2435 (2020).
99. Staal, A. et al. Hysteresis of tropical forests in the 21st century. *Nat. Commun.* **11**, 4978 (2020).
100. O'Connor, J. C., Santos, M. J., Dekker, S. C., Rebel, K. T. & Tuinenburg, O. A. Atmospheric moisture contribution to the growing season in the Amazon arc of deforestation. *Environ. Res. Lett.* **16**, 084026 (2021).
101. Hoek van Dijke, A. J. et al. Shifts in regional water availability due to global tree restoration. *Nat. Geosci.* **15**, 363–368 (2022).
102. Theeuwen, J., Tuinenburg, O., Staal, A., Hamelers, B. & Dekker, S. Moisture recycling in five different regions with Mediterranean climates around the world. *Weather* **1**, 2 (2022).
103. Tuinenburg, O. A., Bosmans, J. H. & Staal, A. The global potential of forest restoration for drought mitigation. *Environ. Res. Lett.* **17**, 034045 (2022).
104. Posada-Marín, J. A., Arias, P. A., Jaramillo, F. & Salazar, J. F. Global impacts of El Niño on terrestrial moisture recycling. *Geophys. Res. Lett.* **50**, e2023GL103147 (2023).
105. Posada-Marín, J. A., Salazar, J. F., Rulli, M. C., Wang-Erlandsson, L. & Jaramillo, F. Global water security risk assessment. *Zenodo* https://doi.org/10.5281/zenodo.11474249 (2024).
106. New, M., Lister, D., Hulme, M. & Makin, I. A high-resolution data set of surface climate over global land areas. *Clim. Res.* **21**, 1–25 (2002).
107. *Harmonized World Soil Database (Version 1.2)* (FAO, 2012).
108. *Groundwater Resources of the World, 1:25,000,000* (BGR/UNESCO, 2012).
109. Portmann, F. T., Siebert, S. & Doll, P. MIRCA2000-global monthly irrigated and rainfed crop areas around the year 2000: a new high-resolution data set for agricultural and hydrological modeling. *Global Biogeochem. Cyc.* **24**, GB1011 (2010).
110. Siebert, K. J., Egi, A. & McCaig, R. Chemometric investigation of barley and malt data. *J. Am. Soc. Brew. Chem.* **70**, 163–175 (2012).
111. Yu, Q. et al. A cultivated planet in 2010—part 2: the global gridded agricultural-production maps. *Earth Syst. Sci. Data* **12**, 3545–3572 (2020).

## Acknowledgements

This work was funded by the Swedish Research Council for Environment, Agricultural Sciences and Spatial Planning (FORMAS) Project 2022-02148, the Swedish Research Council (VR) Project 2021-05774. J.P.-M. was funded by the Colombian Ministry of Science, Technology and Innovation (Minciencias) through the programme 'Excelencia doctoral del Bicentenario' Grant 20230017-25-2020. J.S. was funded by the Colombian Ministry of Science, Technology, and Innovation (Minciencias) through the SOS-Cuenca research programme 'SOStenibilidad de sistemas ecológicos y sociales en la CUENCA Magdalena-Cauca bajo escenarios de cambio climático y pérdida de bosques' (grant no. 1115-852-70719). L.W.-E. was supported by funding from FORMAS (2019-01220, 2022-02089, 2023-0310 and 2023-00321), Horizon Europe (101081661), the IKEA Foundation, the Marianne and Marcus Wallenberg Foundation and the Marcus and Amalia Wallenberg Foundation. The funders had no role in the design, data collection and analysis, decision to publish or preparation of the paper.

## Author contributions

Design: J.P.-M., J.S. and F.J. Project administration and supervision: F.J. Methodology: J.P.-M., J.S. and F.J. Deployment and sampling: J.P.-M. Formal analysis: J.P.-M., J.S., M.C.R., L.W.-E. and F.J. Writing—original draft: J.P.-M., J.S. and F.J. Writing—review and editing: J.P.-M., J.S., M.C.R., L.W.-E. and F.J. Modelling: J.P.-M. and M.C.R. All authors contributed to discussion of the results and the paper.

## Funding

Open access funding provided by Stockholm University.

## Competing interests

The authors declare no competing interests.

## Additional information

**Supplementary information** The online version contains supplementary material available at https://doi.org/10.1038/s44221-024-00291-w.

**Correspondence and requests for materials** should be addressed to José Posada-Marín.

**Peer review information** *Nature Water* thanks Dionysia Panagoulia and the other, anonymous, reviewer(s) for their contribution to the peer review of this work.